Matrix-transmitted paratensile signaling enables myofibroblast–fibroblast cross talk in fibrosis expansion

Longwei Liu[a,b,c,1], Hongsheng Yu[a,1], Hui Zhao[a,b], Zhaozhao Wu[a], Yi Long[a], Jingbo Zhang[a], Xiaojun Yan[a], Zhifeng You[a], Lyu Zhou[a], Tie Xia[d], Yan Shi[d], Bailong Xiao[e], Yingxiao Wang[c], Chenyu Huang[f], and Yanan Du[a,2]

[a]Department of Biomedical Engineering, School of Medicine, Tsinghua-Peking Center for Life Sciences, Tsinghua University, Beijing 100084, China; [b]School of Life Sciences, Tsinghua University, Beijing 100084, China; [c]Institute of Engineering in Medicine, University of California San Diego, La Jolla, CA 92093; [d]Institute for Immunology, School of Medicine, Tsinghua University, Beijing 100084, China; [e]School of Pharmaceutical Sciences, Tsinghua University, Beijing 100084, China; and [f]Department of Dermatology, Beijing Tsinghua Changgung Hospital, School of Clinical Medicine, Tsinghua University, Beijing 102218, China

Edited by Michael P. Sheetz, The University of Texas Medical Branch at Galveston, Galveston, TX, and accepted by Editorial Board Member Yale E. Goldman March 26, 2020 (received for review June 21, 2019)

While the concept of intercellular mechanical communication has been revealed, the mechanistic insights have been poorly evidenced in the context of myofibroblast–fibroblast interaction during fibrosis expansion. Here we report and systematically investigate the mechanical force-mediated myofibroblast–fibroblast cross talk via the fibrous matrix, which we termed paratensile signaling. Paratensile signaling enables instantaneous and long-range mechanotransduction via collagen fibers (less than 1 s over 70 μm) to activate a single fibroblast, which is intracellularly mediated by DDR2 and integrin signaling pathways in a calcium-dependent manner through the mechanosensitive Piezo1 ion channel. By correlating in vitro fibroblast foci growth models with mathematical modeling, we demonstrate that the single-cell-level spatiotemporal feature of paratensile signaling can be applied to elucidate the tissue-level fibrosis expansion and that blocking paratensile signaling can effectively attenuate the fibroblast to myofibroblast transition at the border of fibrotic and normal tissue. Our comprehensive investigation of paratensile signaling in fibrosis expansion broadens the understanding of cellular dynamics during fibrogenesis and inspires antifibrotic intervention strategies targeting paratensile signaling.

mechanical communication | fibrosis propagation | paratensile signaling

Fibrosis is the formation of excess fibrous connective tissue in numerous organs in a reparative response to injury, which is a common pathway to organ damage and failure accounting for up to 50% deaths in the developed world (1, 2). During fibrogenesis, it is widely acknowledged that tissue-resident fibroblasts are activated to myofibroblasts via "paracrine factors" secreted by the recruited immune cells (3). The activated myofibroblasts, with phenotypic changes including cell shape elongation and upregulation of fibrosis-related proteins (e.g., α-SMA, PDGFR-β) compared to fibroblasts (4–6), produce a variety of extracellular matrices (e.g., collagen) and cytokines (e.g., TGF-β), leading to autocrine stimulation of neighboring fibroblasts. Until now, while the contributions of soluble factor-based biochemical cues were well characterized, few biophysical insights have been revealed.

Stiffened extracellular matrix (ECM) with extensive collagen deposition is a hallmark of fibrosis and an outcome of myofibroblast- and fibroblast-mediated matrix production and remodeling (3). Extensive studies have proved that cells can sense and modulate the biophysical properties of the ECM within their resident microenvironment (7, 8), and tension-guided cell matrix reciprocity was demonstrated to orchestrate the fibroblast to myofibroblast transition in macroscopically three-dimensional (3D) microtissues (9). While the concept of mechanical force–mediated intercellular communication has been revealed (*SI Appendix*), the mechanistic insights have been poorly evidenced in the context of myofibroblast–fibroblast interaction during fibrosis expansion.

Here we hypothesize that the contraction force generated by myofibroblasts could be transmitted through the fibrous collagen matrices toward neighboring fibroblasts, resulting in mechanotransduced fibroblasts activation, and the myofibroblast–fibroblast cross talk at the fibrotic border zone could orchestrate the fibroblast foci growth and fibrosis expansion. To distinguish it from paracrine signaling, we term the myofibroblast–fibroblast cross talk mediated by the matrix-transmitted contraction force "paratensile signaling" (Fig. 1).

Results

Paratensile Signaling in Myofibroblast–Fibroblast Cross Talk at the Single-Cell Level. We first visualized the dynamic myofibroblast–fibroblast interactions within the fibrous collagen microenvironment in vitro. Myofibroblasts (TGF-β pretreated fibroblasts) exhibited contractility superior to that of quiescent fibroblasts

Significance

In the context of myofibroblast–fibroblast interaction during fibrosis expansion, the mechanistic insights of intercellular mechanical communication have been poorly evidenced. We systematically investigated the myofibroblast–fibroblast cross talk via the fibrous matrix, which we termed "paratensile signaling" in the context of fibrosis expansion. We experimentally investigated and mathematically modeled the spatiotemporal features of paratensile signaling and revealed the related molecular mechanisms. We showed that paratensile signaling contributes to fibrosis progression and blocking it might potentially attenuate fibrosis expansion. Our comprehensive investigation of paratensile signaling in fibrosis expansion will broaden the understanding of the cellular dynamics during fibrogenesis and inspire paratensile-targeting antifibrotic intervention strategies.

Author contributions: L.L., H.Y., and Y.D. designed research; L.L., H.Y., H.Z., Z.W., Y.L., J.Z., Z.Y., and L.Z. performed research; T.X., Y.S., B.X., Y.W., and C.H. contributed new reagents/analytic tools; L.L., H.Y., H.Z., and Y.L. analyzed data; and L.L., H.Y., and X.Y. wrote the paper.

The authors declare no competing interest.

This article is a PNAS Direct Submission. M.P.S. is a guest editor invited by the Editorial Board.

[1]L.L. and H.Y. contributed equally to this work.

[2]To whom correspondence may be addressed. Email: duyanan@tsinghua.edu.cn.

This article contains supporting information online at https://www.pnas.org/lookup/suppl/doi:10.1073/pnas.1910650117/-/DCSupplemental.

First published May 1, 2020.

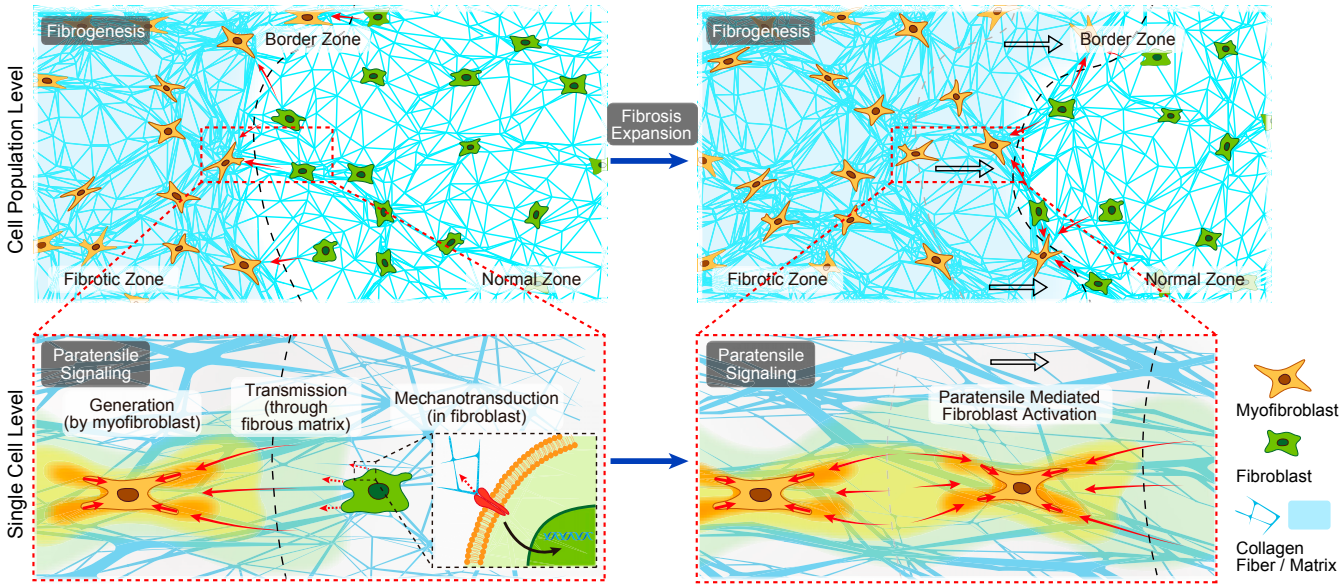

Fig. 1. Schematic illustration defining the hypothesis of paratensile signaling in fibrosis expansion. Conceptual illustration of single-cell-level intercellular paratensile signaling in fibrosis expansion, which mainly involves three stages, including 1) force generation by a myofibroblast, 2) force transmission through the fibrous matrix, and 3) mechanotransduction in a receiving a fibroblast nearby.

(maximum stress of 400 vs. 80 Pa, *SI Appendix*, Fig. S1 *G* and *H*), as illustrated by a greater capacity for matrix deformation in the microbead displacement assay (Fig. 2*A* and *SI Appendix*, Fig. S1 *B* and *C*). When randomly cocultured, a single myofibroblast could activate neighboring fibroblasts within an effective distance of ~200 μm (Fig. 2 *B* and *C* and *SI Appendix*, Fig. S2), and a single myofibroblast cluster (containing ~30 myofibroblasts) could extend the effective distance to >300 μm (*SI Appendix*, Fig. S3) in 6 h. The myofibroblast condition medium was unable to activate the quiescent fibroblasts, indicating paracrine factors secreted by myofibroblasts alone were not sufficient to induce fibroblast activation (Fig. 2*C*).

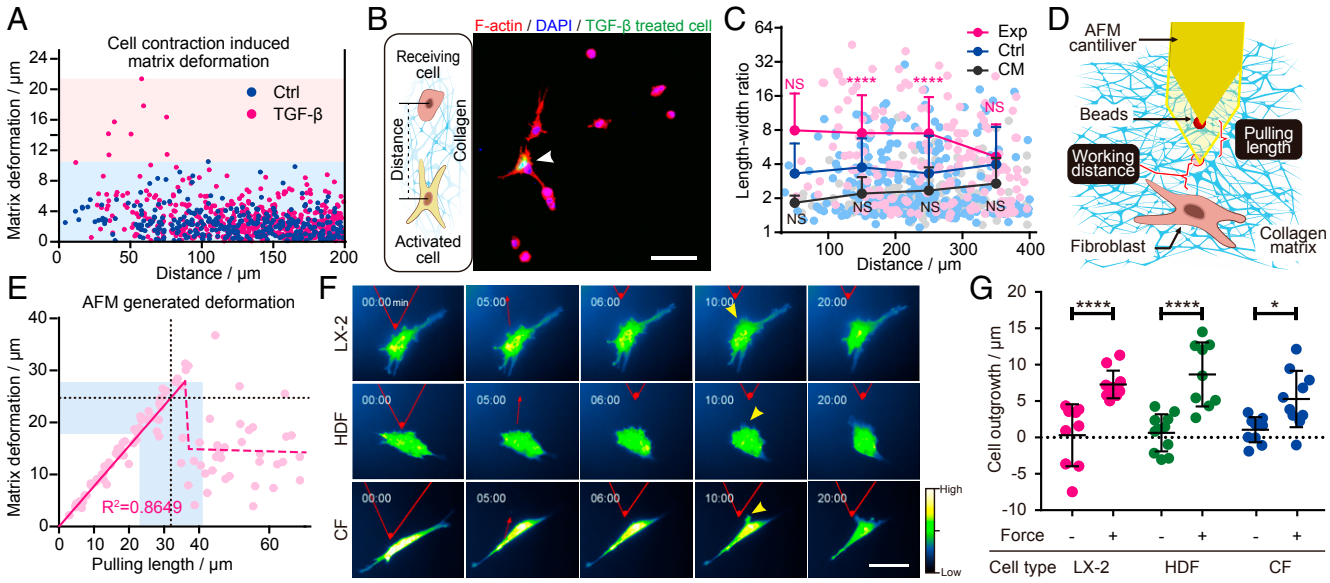

Fig. 2. Single-cell-level intercellular paratensile signaling in vitro. (*A*) Collagen matrix deformation induced by a single fibroblast before and after TGF-β activation measured by the microbead displacement assay. (*B*) Immunofluorescent images of F-actin on a collagen matrix. Arrowhead, TGF-β pretreated cells labeled with CellTracker Green. (Scale bar, 100 μm.) (*C*) Length–width ratio of neighboring fibroblasts located at various distances from TGF-β–activated fibroblasts (Exp, magenta dots, $n = 172$, two-way ANOVA, $^{****}P < 0.0001$), randomly selected normal fibroblasts (Ctrl, blue dots, $n = 258$), and randomly selected normal fibroblasts cultured in condition medium (CM, black dots, $n = 152$, two-way ANOVA; NS, not significant). (*D*) Schematic illustration of AFM-based paratensile stimulation at the single-cell level. (*E*) Collagen matrix deformation quantified by bead displacement in the AFM experiment with different pulling lengths at a distance of 10 μm. The dashed black line and light blue area illustrate the pulling length and matrix deformation applied in *F* and *G*. (*F*) Representative images of dynamic changes in actin in a single fibroblast from multiple tissue origins over the course of an experiment (cells were stretched for 15 min after 5 min of observing without stretching as a self-control). HDF, human dermal fibroblast; CF, cardiac fibroblast. (Scale bar, 50 μm.) (*G*) Quantitative analysis of the lengths of actin outgrowths before and after paratensile stimulation shown in *F* ($n \geq 9$, two-way ANOVA, $^{****}P < 0.0001$, $^{*}P = 0.0147$). See also Movie S2. Data are expressed as mean ± SD.

Decoupling the paracrine signaling and paratensile signaling in intercellular interactions during in vitro culture was a challenge (10). To solve this problem, we developed an atomic force microscope (AFM)-based single-cell paratensile stimulation platform (Fig. 2*D* and *SI Appendix*, Fig. S1 *D* and *E*) to verify the response of cells to a collagen-transmitted paratensile signal. A tension force mimicking the matrix-transmitted force generated by a single myofibroblast contraction (Fig. 2*A*) was applied to the targeted fibroblast via AFM tip–induced matrix deformation (Fig. 2*E*). Fibroblasts from the liver, heart, and skin transfected with an actin reporter were subjected to paratensile stimulation and monitored under the microscope for phenotypic changes. Fibroblasts from all of the tissue types were responsive to paratensile stimulation as indicated by significant actin polymerization and outgrowth of stress actin fibers toward the direction of the force (Fig. 2 *F* and *G* and *SI Appendix*, Fig. S4). These results indicate that the paratensile signaling can mediate the intercellular cross talk between a myofibroblast and the adjacent fibroblast at the single-cell level.

Transmission Distance of Paratensile Signaling. Next, the spatial features of paratensile signals including the response time and working distance were investigated. When a pulling force to mimic the cell contraction of a single myofibroblast (with a pulling length of ~40 μm, *SI Appendix*, Figs. S1–S5) was applied, the matrix-transmitted paratensile signal could induce significant outgrowth of actin fibers in fibroblasts at a distance of 30 μm (Fig. 3 *A* and *B*). However, a pulling force mimicking fibroblast contraction (with a pulling length of ~20 μm, *SI Appendix*, Fig. S5) only exhibited an effective transmission distance of about 10 μm (Fig. 3 *A* and *B*), indicating the dominant role played by myofibroblasts in myofibroblast–fibroblast cross talk. Meanwhile, the effective transmission distance could reach as high as 70 μm when the cells were cultured on remodeled collagen (*SI Appendix*, Fig. S6). Meanwhile, no obvious force activation was

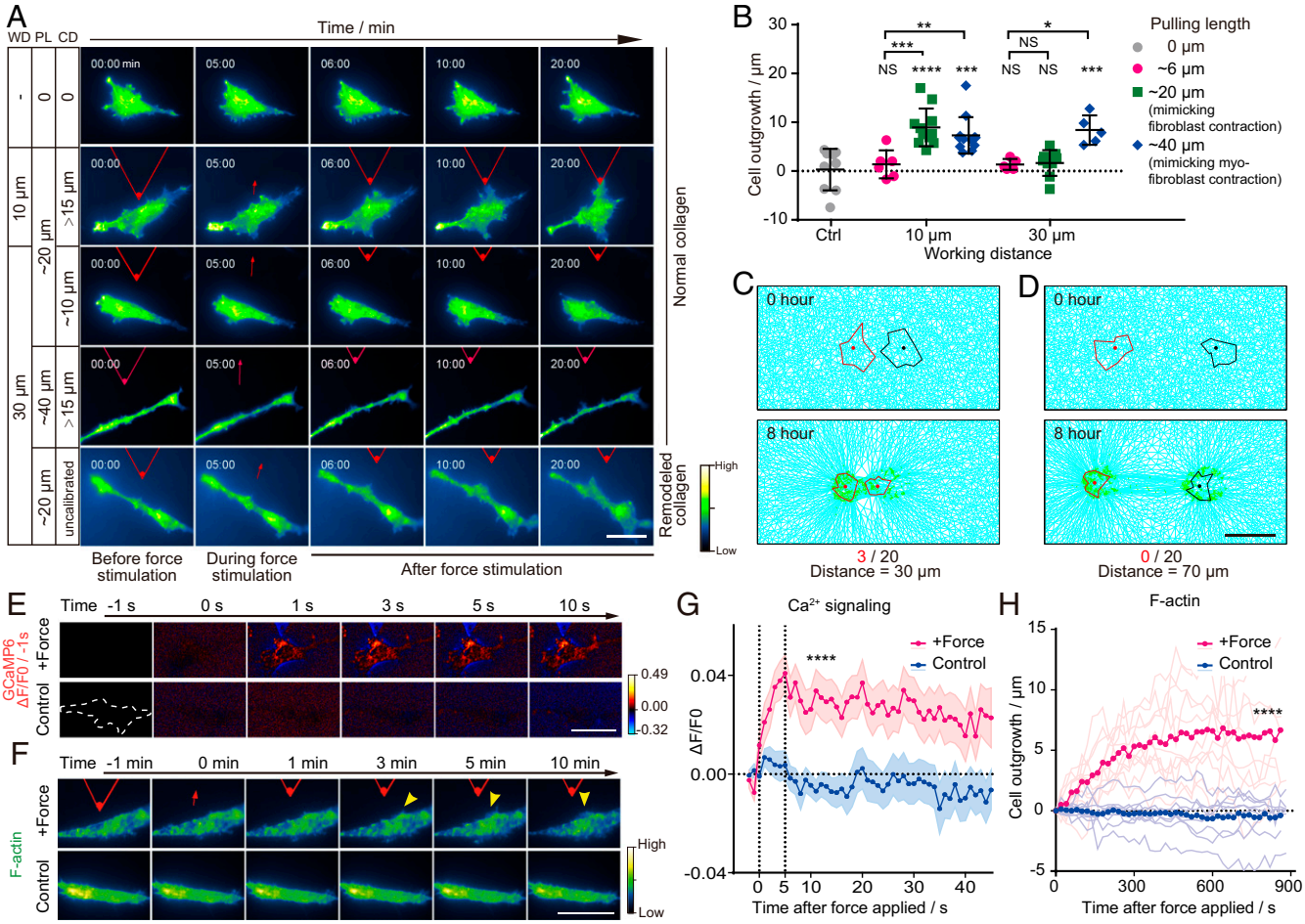

Fig. 3. Transmitting distance and response time of cells to paratensile signaling. (*A*) Representative images of dynamic changes in F-actin in fibroblasts (LX2) under different pulling lengths (PL), working distances (WD), and collagen deformation (CD) at the boundary of a fibroblast. (Scale bar, 50 μm.) See also Movie S3. (*B*) Quantitative analysis of the lengths of actin outgrowths before and after paratensile stimulation in *A* ($n \geq 6$ as indicated, two-way ANOVA; from left to right and top to bottom, $^{**}P = 0.0079$, $^{*}P = 0.0139$, $^{***}P = 0.0005$, NS $P = 0.9989$, NS $P = 0.9366$, $^{****}P < 0.0001$, $^{***}P = 0.0002$, NS $P = 0.9509$, NS $P = 0.8531$, and $^{***}P = 0.0008$, respectively; NS, not significant). (*C*) In silico modeling of cell activation by paratensile signaling applied by a neighboring cell with a spacing distance of 30 μm (3 activations out of 20 simulations). (*D*) No cells could be activated by paratensile signaling when the simulated spacing distance was increased to 70 μm (0 activations out of 20 simulations). (Scale bar, 50 μm.) See also Movie S4. (*E*) Representative images of calcium changes in LX2 after paratensile stimulation. (Scale bar, 50 μm.) See also Movie S5. (*F*) Representative images of actin remodeling in LX2 after paratensile stimulation. (Scale bar, 50 μm.) See also Movie S5. (*G*) Dynamic changes in the calcium signal after paratensile stimulation. Magenta and blue areas indicate the mean ± SEM in each group ($n = 30$ in each group, Student's *t* test, $^{****}P < 0.0001$). (*H*) Dynamic changes in actin outgrowth after paratensile stimulation. Each light magenta (force stimulation) or light blue (control) line indicates one replicate in each group ($n \geq 11$ in each group, Student's *t* test, $^{****}P < 0.0001$). Data are expressed as mean ± SD.

observed even with a working distance of 10 μm on a nonfibrous matrix (i.e., gelatin hydrogel, *SI Appendix*, Fig. S7). To simulate the paratensile signaling and decouple the paracrine factors, a myofibroblast–fibroblast populated collagen lattice (FMPCL) model was established in which only the paratensile signaling was taken into consideration within the intercellular communication (*SI Appendix*, *Materials and Methods*) based on a previous model (11). The FMPCL model could nicely recapture the effective transmission distance (~30 μm) of paratensile signaling obtained in the in vitro experiment, while no fibroblast activation could be found in stimulation when the transmission distance was increased to 70 μm (Fig. 3 *C* and *D* and *SI Appendix*, Fig. S11).

The Response Time of Fibroblast Activation to Paratensile Signaling. After that, the timescale of paratensile signaling and the molecular mechanism of mechanotransduction in receiving cells were explored. Calcium was previously reported to participate in mechanosensing and to influence actin polymerization (12, 13). When cells were subjected to paratensile stimulation, calcium influx into the cytoplasm was observed after less than a second and plateaued after ~5 s, indicating that cells responded instantaneously to paratensile stimulation (Fig. 3 *E* and *G*). Actin polymerization was prominent after 2 min and stabilized within 10 min (Fig. 3 *F* and *H*). Paratensile-induced mechanotransduction could then activate the fibroblasts by up-regulating fibrogenic expression of α-SMA within ~40 min (*SI Appendix*, Fig. S12). These results indicate that the response of fibroblasts to paratensile stimulation is rapid and well orchestrated.

Intracellular Mechanotransduction of Paratensile Signaling. Next, downstream mechanotransduction mediators of paratensile signaling were investigated. Integrins and discoidin domain receptors (DDRs) are two major types of collagen receptors that mediate cell–matrix interactions. We found that targeting either integrin β1 or DDR2 could significantly attenuate paratensile-induced actin remodeling (*SI Appendix*, Figs. S13 *A* and *B* and S14). FAK, PI3K, and AKT were previously reported to be common downstream effectors of integrin/DDR signaling pathways. These effectors control actin polymerization (14, 15) by modulating the Arp2/3 complex (16, 17), which leads to the translocation of myocardin-related transcription factor (MRTF), mainly MRTF-A (also known as MLK1) on a fibroblast background, to the nucleus where it initiates α-SMA transcription (18, 19). As expected, inhibitors targeting these downstream effectors of the integrin/DDR signaling pathways significantly reduced actin remodeling (*SI Appendix*, Fig. S13 *A* and *B*). Furthermore, blocking calcium influx with the EGTA significantly inhibited actin outgrowth, indicating the indispensable role of calcium influx in paratensile mechanotransduction. Since the mechanosensitive cation channel Piezo (20) was previously reported to gate calcium influx in response to mechanical stimuli, we knocked down Piezo1 in fibroblasts, and these cells lost Ca^{2+} responsiveness and the subsequent actin remodeling to paratensile-mediated stimulation (*SI Appendix*, Figs. S13*C*, S15, and S16). Downstream of calcium signaling, MLCK was reported to be activated upon the binding of Ca^{2+} to calmodulin and to control F-actin assembly by modulating myosin activity (21). We then verified the involvement of this pathway in paratensile signaling by blocking active MLCK, which hampered F-actin remodeling within receiving cells (*SI Appendix*, Fig. S13 *A* and *B*). Collectively, these results demonstrate that interplay between the Piezo1–Ca^{2+}–MLCK signaling pathway and the DDR2/integrin–FAK–PI3K/AKT–Arp2/3 signaling pathways might synergistically govern mechanotransduction of paratensile signals to regulate cytoskeletal actin polymerization and downstream MRTF nucleus translocation, leading to the promotion of α-SMA gene expression in receiving cells (*SI Appendix*, Fig. S13*D*).

Long-Term Paratensile Signaling Mediated Myofibroblast–Fibroblast Cross Talk at the Border Zone of the Fibrotic Tissue Model. Next, the role of paratensile signaling in long-term myofibroblast–fibroblast cross talk was investigated at the border zone of an in vitro fibrotic tissue model (Fig. 4*A*), which was intended to recapitulate the fibroblast foci growth during fibrosis. The in vitro fibrotic tissue model was established using PDGFR-β-reporter dermal fibroblasts, which were isolated from the dermis of a C57BL/6-Ai14(RCL-tdT)-D;Pdgfrbtm1(iCre) mouse. Up-regulation of the PDGFR-β-tdTomato reporter was reported previously to represent the activation of fibroblast to myofibroblast and colocalize with α-SMA (*SI Appendix*, Fig. S17) (22). Dynamic changes in myofibroblast and fibroblast cellular distribution and fibroblast activation were characterized at the border zone between fibrotic (myofibroblast area) and normal tissue (fibroblast area) (Fig. 4*B* and *SI Appendix*, Fig. S18). Meanwhile, to rule out the influence of paracrine factors, a multicellular FMPCL in silico model (*SI Appendix*, *Materials and Methods*) was established based on the spatiotemporal features of paratensile signaling, which could well recapitulate myofibroblast–fibroblast interactions mediated only by force transmission through condensed collagen fibers (Fig. 4*C*). Statistical analyses of both in vitro and in silico models indicate significant propagation of activated fibroblast toward normal tissue, which could be significantly attenuated by blocking paratensile signaling (Fig. 4 *F*–*I*). These results were consistent with the previous conclusion that paracrine signaling alone was not sufficient to induce fibroblast activation (Fig. 2*C*). It should be noted that the directional cell migration of myofibroblasts is much slower than the propagation speed of fibroblast activation (4 ± 7 vs. 41 ± 26 μm/h in the in vitro model), which rules out the significant contribution of myofibroblast migration to the activated fibroblast expansion (fibroblast foci growth) (Fig. 4*D*). Obvious collagen remodeling was found at the border zone and could be restrained after blocking paratensile signaling in the in vitro model (Fig. 4*E*). These results demonstrate that the spatiotemporal features of paratensile signaling we concluded from the single-cell level could be applied to describe the cell population behavior of fibroblasts at the border zone mimicking fibroblast foci growth during fibrosis expansion.

Paratensile Signaling in Fibrosis Expansion. Besides the role of paratensile signaling in fibroblast foci growth, we further explored the contribution of paratensile signaling to fibrosis expansion in in vitro and in silico models recreating the dynamic changes of architectural features, myofibroblast and fibroblast distribution, and collagen remodeling during cardiac fibrosis progression. In these models, myofibroblasts and fibroblasts were initially patterned as neighbors embedded within ringlike collagen gels (each with a width of 4 mm) to mimic their distribution in a cross section of a fibrotic rat myocardium (Fig. 5*A* and *SI Appendix*, Fig. S19). Dynamic changes in pathogenic phenotypes observed during fibrosis expansion in vivo such as left ventricular wall thinning due to myocardium remodeling (23) (*SI Appendix*, Fig. S19) could be partially recapitulated by both the in vitro and in silico models of cardiac fibrosis (Fig. 5 *B* and *C*). To precisely characterize these dynamics, half contraction angles (Fig. 5*A*) were quantified during the entire tissue remodeling process, and similar patterns were observed for fibrosis expansion in silico (solely mediated by paratensile signaling) and in vitro (Fig. 5 *K* and *L*). Intercellular interactions led to spatial heterogeneity in the resulting fibrotic tissues, and these regions were defined as fibrotic, border, and remote zones (Fig. 5 *A*, *D*, and *E*). In both models, the border zone with myofibroblasts was quickly remodeled, followed by the much faster shrinkage of the left ring of the microtissue (as illustrated by changes in contraction angles) compared to the control group (*SI Appendix*, Fig. S20). Furthermore, tissue stiffening (*SI Appendix*, Fig. S21) and collagen condensation (Fig. 5*F*) were found to be more prominent in the fibrotic zone in the in vitro fibrosis tissue model, in line with the spatial distribution

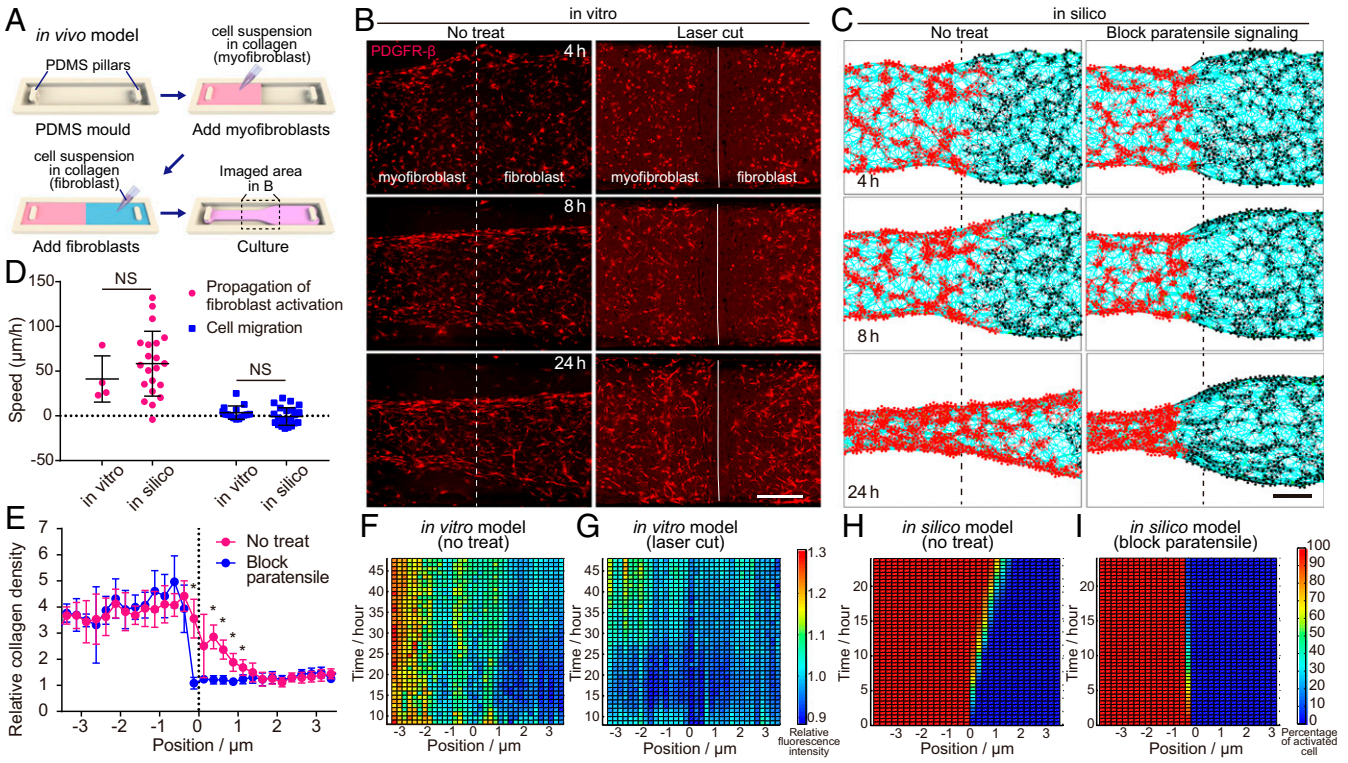

Fig. 4. Fibrosis expansion from the border zone mediated by paratensile signaling in vitro and in silico. (*A*) Schematic illustration of procedures to establish in vitro models to investigate fibrosis expansion. (*B* and *C*) Live imaging of fibroblast activation status indicated by PDGFR-β expression in the in vitro fibrosis models with and without laser cut to block paratensile signaling transmitting in the collagen matrix (*B*), which is well predicted by the paratensile-based mathematical model (*C*). (Scale bar, 5 mm.) The white solid line indicates the border line between the myofibroblast and fibroblast, while white dashed line indicates the route of laser cutting in *B*. See also Movie S6. (*D*) Quantification of the propagation speed of fibroblast activation and migration speed of activated fibroblasts both in vitro and in silico ($n \geq 4$, Student's *t* test, from left to right, NS $P = 0.3813$, NS $P = 0.1390$; NS, not significant). (*E*) Quantification of collagen density in in silico models after 24 h of simulated remodeling ($n = 8$, Student's *t* test, $^*P < 0.05$). (*F* and *G*) Heat maps illustrating the spatial–temporal distribution of relative fluorescence intensity in the in vitro model with (*F*) and without (*G*) laser cut treatment. (*H* and *I*) Heat maps illustrating the spatial–temporal distribution of activated fibroblasts in the in silico model with (*I*) and without (*H*) paratensile signaling blocking. Data are expressed as mean ± SD.

of remodeled collagen during fibrosis expansion in vivo (*SI Appendix*, Fig. S21*A*). Simulation of fibrosis expansion solely mediated by paratensile signaling without any paracrine factor could also well recapitulate the collagen remodeling process in vitro and in vivo, as demonstrated by the increased collagen density in the fibrotic zone compared with other regions (Fig. 5 *E* and *H*). At the cellular level, a gradient in the ratio of myofibroblasts to fibroblasts was observed across the three zones both in silico (Fig. 5*I*) and in vitro (Fig. 5*G*), with higher cellular F-actin and α-SMA expression in the fibrotic zone. Taken together, these results demonstrate that the solely paratensile based in silico model nicely recapitulates the phenotypes of fibrosis expansion observed in vitro and in vivo, indicating that paratensile signaling–mediated myofibroblast–fibroblast cross talk plays an indispensable role in fibrosis expansion.

Therapeutic Intervention by Targeting Paratensile Signaling. To explore whether blocking paratensile signaling could potentially attenuate fibrosis expansion, multiple antiparatensile strategies were theoretically predicted and experimentally verified. Reduction of force transmission with the collagen crosslinking enzyme (LOX) inhibitor BAPN and blockage of integrin-mediated mechanotransduction signaling with the RGD peptide both significantly prevented fibrosis expansion in vitro (Fig. 5 *J* and *K*). These effects could be precisely predicted by theoretical simulations (Fig. 5 *J* and *L*). It should be noted that the therapeutic efficacy of the LOX inhibitor BAPN for cardiac fibrosis treatment in in vivo rat models was verified in a previous study (24). We also targeted MKL1, a key mechanoresponsive transcription factor in the MRTF family, which translocates into the nucleus to activate α-SMA expression (18). MKL1 showed strong nuclear localization in the fibrotic zone, and blockage of the MKL1 signaling pathway attenuated fibrosis expansion (*SI Appendix*, Fig. S22). These results demonstrate that the in vitro and in silico 3D cardiac fibrosis models could potentially be utilized as platforms for testing compounds targeting paratensile signaling, which might uncover unique mechanisms of action for future antifibrosis therapy.

Conclusions

Here we systematically investigated the spatiotemporal features of the fibrous matrix-transmitted myofibroblast–fibroblast cross talk in the context of fibrosis expansion, which we termed paratensile signaling. We proved that paratensile signaling could enable fibroblast to myofibroblast transition mediated by collagen fiber-transmitted force both in silico and in vivo and outlined the main principles of paratensile signaling, which involve three major phases, namely, contractile force generation by the myofibroblast, force transmission through the fibrous extracellular matrix, and intracellular mechanotransduction in the adjacent fibroblast (Fig. 1 and Movie S1). Spatiotemporal features of the paratensile signaling at the single-cell level and tissue level were systematically investigated, which provided insights into regulatory and responsive molecular mechanisms. Meanwhile, by constructing in vitro and in silico pathological tissue models, we showed that the paratensile signaling could contribute to fibrosis progression and blocking paratensile signaling might potentially attenuate fibrosis expansion. However, several important parameters, including bending stiffness, nonlinearity, and the nodal coordination number of collagen fibers (25, 26), have not been taken

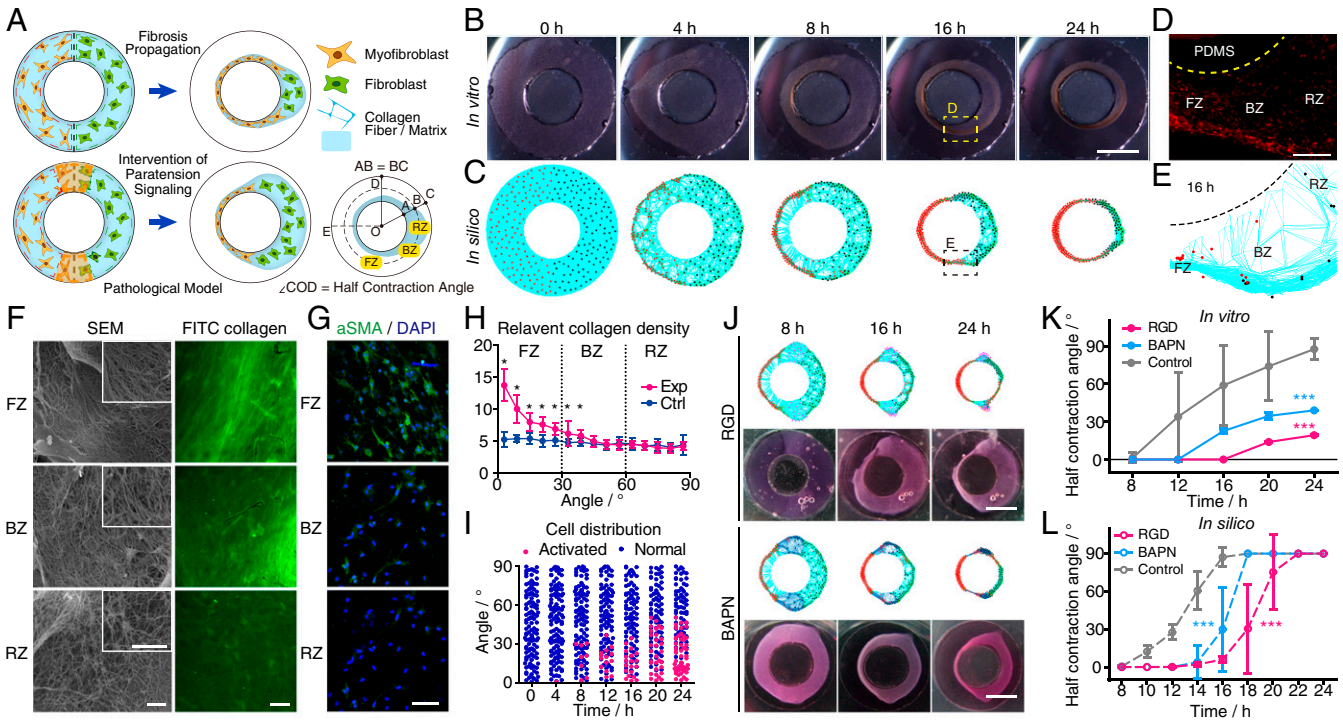

Fig. 5. Paratensile-mediated fibrosis expansion in in vitro and in silico cardiac fibrosis models. (*A*) Design of the in vitro cardiac fibrosis model, which recapitulates the ventricular cross-sectional geometry and distribution of myofibroblasts and fibroblasts. (*B* and *C*) Live imaging of tissue remodeling in the in vitro cardiac fibrosis models (*B*), which is well predicted by the paratensile-based mathematical model (*C*). FZ, fibrotic zone, BZ, border zone, RZ, remote zone. (Scale bar, 5 mm.) See also Movie S7. (*D*) Spatial heterogeneity in the myofibroblast distribution within the three zones of the in vitro cardiac fibrosis model in *B* after 16 h. Red fluorescence represents fibroblasts expressing the α-SMA reporter. PDMS, polydimethylsiloxane. (Scale bar, 500 μm.) (*E*) Representative image of cardiac fibrosis in the in silico model at 16 h. (*F*) SEM and confocal images of collagen fibers in different zones indicate extensive remodeling of collagen fibers in the FZ. (Scale bar, 5 μm in SEM images and 200 μm in confocal images.) (*G*) Activated myofibroblasts in the three zones of the in vitro models were characterized by immunofluorescent staining of α-SMA. (Scale bar, 50 μm.) (*H*) Quantification of collagen density in in silico models after 16 h of simulated remodeling. See also Movie S7*A* for the control. The angle shown on the x axis is the angle between OC and OD (∠COD) in *A* ($n = 10$, Student's *t* test, $^*P < 0.05$). (*I*) Quantification of the number and spatial distribution of activated myofibroblasts during simulated cardiac fibrosis expansion. (*J*) Inhibition of collagen receptor signaling and collagen remodeling slowed down fibrosis expansion, which was verified by multicellular mathematical models. (Scale bar, 5 mm.) See also Movie S8. (*K* and *L*) Dynamic changes in the half contraction angle with and without inhibition of paratensile signaling in vitro ($n \geq 4$ in each group) and in silico ($n = 10$ in each group, two-way ANOVA, $^{***}P < 0.001$). Data are expressed as mean ± SD.

into consideration in the current in silico models, which may limit the interpretation of the simulation results. These factors will be taken into consideration in future model optimization to obtain more accurate predication (*SI Appendix*). Further investigations into paratensile signaling will broaden our understanding of the cellular dynamics during fibrogenesis and inspire paratensile-targeting intervention strategies to battle fibrosis diseases (*SI Appendix*).

Materials and Methods

All experimental procedures, including cell culture, primary cell isolation, myofibroblast–fibroblast interaction on the collagen matrix, cell stretching, cell contraction force characterization, AFM-applied mechanical stimulation, mathematical models, in vitro fibrosis models, animal experiments, and statistical analyses are presented in *SI Appendix, Materials and Methods*.

Data Availability Statement. The data supporting the findings of this study are available within the paper and its *SI Appendix*.

ACKNOWLEDGMENTS. We would like to acknowledge the Laboratory Animal Research Center and Center of Biomedical Analysis at Tsinghua University for technical assistance. This work is financially supported by the Beijing Natural Science Foundation (grant no. JQ18022), the Beijing Municipal Science & Technology Commission (grant no. Z181100001818005), and the National Natural Science Foundation of China (grant no. 31671036).

1. S. L. Friedman, D. Sheppard, J. S. Duffield, S. Violette, Therapy for fibrotic diseases: Nearing the starting line. *Sci. Transl. Med.* **5**, 167sr1 (2013).
2. D. C. Rockey, P. D. Bell, J. A. Hill, Fibrosis–A common pathway to organ injury and failure. *N. Engl. J. Med.* **373**, 96 (2015).
3. J. S. Duffield, M. Lupher, V. J. Thannickal, T. A. Wynn, Host responses in tissue repair and fibrosis. *Annu. Rev. Pathol.* **8**, 241–276 (2013).
4. S. Asano *et al.*, Matrix stiffness regulates migration of human lung fibroblasts. *Physiol. Rep.* **5**, e13281 (2017).
5. N. C. Henderson *et al.*, Targeting of αv integrin identifies a core molecular pathway that regulates fibrosis in several organs. *Nat. Med.* **19**, 1617–1624 (2013).
6. J. J. Tomasek, G. Gabbiani, B. Hinz, C. Chaponnier, R. A. Brown, Myofibroblasts and mechano-regulation of connective tissue remodelling. *Nat. Rev. Mol. Cell Biol.* **3**, 349–363 (2002).
7. S. Checa, M. K. Rausch, A. Petersen, E. Kuhl, G. N. Duda, The emergence of extracellular matrix mechanics and cell traction forces as important regulators of cellular self-organization. *Biomech. Model. Mechanobiol.* **14**, 1–13 (2015).
8. A. J. Engler, S. Sen, H. L. Sweeney, D. E. Discher, Matrix elasticity directs stem cell lineage specification. *Cell* **126**, 677–689 (2006).
9. P. Kollmannsberger, C. M. Bidan, J. W. C. Dunlop, P. Fratzl, V. Vogel, Tensile forces drive a reversible fibroblast-to-myofibroblast transition during tissue growth in engineered clefts. *Sci. Adv.* **4**, eaao4881 (2018).
10. L. Sapir, S. Tzlil, Talking over the extracellular matrix: How do cells communicate mechanically? *Semin. Cell Dev. Biol.* **71**, 99–105 (2017).
11. J. C. Dallon, E. J. Evans, H. P. Ehrlich, A mathematical model of collagen lattice contraction. *J. R. Soc. Interface* **11**, 20140598 (2014).
12. X. Shao, Q. Li, A. Mogilner, A. D. Bershadsky, G. V. Shivashankar, Mechanical stimulation induces formin-dependent assembly of a perinuclear actin rim. *Proc. Natl. Acad. Sci. U.S.A.* **112**, E2595–E2601 (2015).
13. J. Gergely, Ca2+ control of actin-myosin interaction. *Basic Res. Cardiol.* **75**, 18–25 (1980).
14. L. S. Payne, P. H. Huang, Discoidin domain receptor 2 signaling networks and therapy in lung cancer. *J. Thorac. Oncol.* **9**, 900–904 (2014).

15. B. Leitinger, Transmembrane collagen receptors. *Annu. Rev. Cell Dev. Biol.* **27**, 265–290 (2011).
16. H. E. Johnson *et al.*, F-actin bundles direct the initiation and orientation of lamellipodia through adhesion-based signaling. *J. Cell Biol.* **208**, 443–455 (2015).
17. E. D. Goley, M. D. Welch, The ARP2/3 complex: An actin nucleator comes of age. *Nat. Rev. Mol. Cell Biol.* **7**, 713–726 (2006).
18. R. Pawłowski, E. K. Rajakylä, M. K. Vartiainen, R. Treisman, An actin-regulated importin α/β-dependent extended bipartite NLS directs nuclear import of MRTF-A. *EMBO J.* **29**, 3448–3458 (2010).
19. E. N. Olson, A. Nordheim, Linking actin dynamics and gene transcription to drive cellular motile functions. *Nat. Rev. Mol. Cell Biol.* **11**, 353–365 (2010).
20. B. Coste *et al.*, Piezo proteins are pore-forming subunits of mechanically activated channels. *Nature* **483**, 176–181 (2012).
21. L. Follonier Castella, G. Gabbiani, C. A. McCulloch, B. Hinz, Regulation of myofibroblast activities: Calcium pulls some strings behind the scene. *Exp. Cell Res.* **316**, 2390–2401 (2010).
22. Y. T. Chen *et al.*, Platelet-derived growth factor receptor signaling activates pericyte-myofibroblast transition in obstructive and post-ischemic kidney fibrosis. *Kidney Int.* **80**, 1170–1181 (2011).
23. M. G. Sutton, N. Sharpe, Left ventricular remodeling after myocardial infarction: Pathophysiology and therapy. *Circulation* **101**, 2981–2988 (2000).
24. J. González-Santamaría *et al.*, Matrix cross-linking lysyl oxidases are induced in response to myocardial infarction and promote cardiac dysfunction. *Cardiovasc. Res.* **109**, 67–78 (2016).
25. C. P. Broedersz, F. C. MacKintosh, Modeling semiflexible polymer networks. *Rev. Mod. Phys.* **86**, 995–1036 (2014).
26. R. C. Picu, Mechanics of random fiber networks—A review. *Soft Matter* **7**, 6768–6785 (2011).